Nuclear Magnetic Shielding of Monoboranes. Calculation and Assessment of ^{11}B NMR Chemical Shifts in Planar BX_3 and in Tetrahedral $[BX_4]^-$ Systems

Jan Macháček, [†] Michael Bühl, [‡] Jindřich Fanfrlík, [§] and Drahomír Hnyk*,[†]

[†]Institute of Inorganic Chemistry of the Czech Academy of Sciences, v.v.i., CZ -250 68 Husinec - Řež, Czech Republic

[‡]School of Chemistry, North Haugh, University of St. Andrews, St. Andews, Fife, KY16 9ST, UK

[§]Institute of Organic Chemistry and Biochemistry of the Czech Academy of Sciences, Flemingovo nám. 2, CZ -166 10 Prague 6, Czech Republic

■ **AUTHOR INFORMATION**

Corresponding Author

hnyk@iic.cas.cz (D.H.)

ABSTRACT:

^{11}B NMR chemical shifts of tricoordinated BX_3 and tetracoordinated BX_4^- compounds (X = H, CH_3, F, Cl, Br, I, OH, SH, NH_2, and CH=CH_2) were computed and the shielding tensors were explored not only within the nonrelativistic GIAO approach but also by applying both relativistic ZORA computations including spin-orbit coupling as well as by employing scalar nonrelativistic ZORA computations (BP86 level of density functional theory). The contributions of the spin-orbit coupling to the overall shieldings are decisive for X = Br and I in both series. No relationship was found between the 2p orbital occupancies or $1/\Delta E$ (difference between LUMO and suitably occupied MO that can be coupled with LUMO) with the shielding tensors (or their principal values) in the BX_3 series. However, a multidimensional statistical approach known as factor analysis (frequently used in chemometrics) revealed that three factors account for 92 % of the cumulative proportion of total variance. The main components of the first factor are occupancies in the $2p_x$ and $2p_y$ orbitals and $1/\Delta E$, the second factor is mainly the occupancy in the $2p_z$ orbital and the inductive substituent parameters by Taft and, finally, the third factor consists exclusively (99.3 %) of the electrostatic potentials (V_{max}), which is directly related to the so-called π-hole magnitudes.

■ INTRODUCTION

Molecular and electronic structures of various types of cluster boranes and heteroboranes (multicenter 3c2e bonding)[1] have recently become the focus of many studies, both experimental and theoretical.[3,4] In particular, the so-called *ab initio* (or DFT)/IGLO (or GIAO)/NMR approach has been repeatedly applied for such purpose.[3,4] The proposed structure of a cluster, usually on the basis of experimental ^{11}B NMR spectra,[5] is optimized at a correlated *ab inito* level, or employing a DFT method. Resulting minima are subsequently subject to magnetic properties calculations using IGLO- or GIAO-based methods in non-relativistic or relativistic (e.g. ZORA) implementations.[3,4] The degree of agreement between the calculated and experimental $\delta(^{11}B)$ serves as a criterion of the correctness of the cluster geometry in solution. For some cases the necessity of employing dynamic electron correlation in computing shielding tensor is obvious.[6] Evidently, the shielding constant of an individual boron nucleus within the cluster molecule is influenced by the interaction with the other boron atoms that are present. There were attempts to assess substitution NMR effects in various cluster compounds by means of regression analysis.[7,8] However, the number of substituents bonded to a boron atom within a cluster was quite limited and physical meanings of the obtained constants from these linear regressions were more or less guessed. However, there exists a greater variety of substituents that are bonded to a *single boron* atom, i.e. without considering the influence of any other boron nuclei. Similar assessments as mentioned above might provide a further insight into understanding of behaviour of ^{11}B (and ^{10}B) nuclei in a magnetic field.[9] The systematic study of BX_3 and $[BX_4]^-$ systems (described with classical 2c2e Lewis structures, see Figure 1 for the molecular diagrams) employing the above mentioned model chemistries might further contribute to such an understanding. Since the BX_3 systems are richer in terms of variety of substituents bonded to B than in systems with more boron atoms, a more sophisticated statistical approach can be applied for assessment of NMR substitution effects.

A few ^{11}B NMR examinations of halogenated boron atoms with such trigonal and tetrahedral structural motifs with D_{3h} and T_d symmetries, respectively, have been already carried out.[10-12] The importance of the spin-orbit coupling,[13-14] σ_{SO}, was recognised for X = Br, I.[10,11] This effect contributes to the overall shielding; in a non-relativistic framework the latter is mainly rationalized as a sum of the diamagnetic, σ_d, and paramagnetic, σ_p,contributions, to which spin-orbit contributions, σ_{SO} ,can be added in a corresponding relativistic treatment. In the absence of strong spin-orbit effects it is the paramagnetic deshielding contribution that accounts for most of the shielding changes. The classical Ramsey equation[15-16] is a simplified relation that attempts to interpret this paramagnetic term in an atom-in-a-molecule approach as being dependent on the mean excitation energy (in other words the energy gap between LUMO and suitable occupied MOs as described below), on the inverse cube roots of the mean expectation values for the *p* and *d* orbital distances from the nucleus, and on the degree of imbalance of valence electrons in the corresponding orbitals. It leads to the downfield shift caused by the coupling of suitable occupied and unoccupied orbitals by the perturbation of the applied magnetic field.[17-19] In contrast, the diamagnetic shielding leads to an upfield shift and is derived from just the ground-state charge distribution.

Apart from D_{3h}-symmetrical boron trihalides, BX_3, and T_d-symmetrical tetrahaloborates (X = F, Cl, Br, I),[20] there exist further substituents that are able to coordinate B in both series, resulting in symmetries different from D_{3h} and T_d. The experimental ^{11}B NMR chemical shifts in the corresponding pairs differ significantly, similarly as in the halogen-containing BX_3 /BX_4^- pairs:[21] the B-atom in a tri-coordinated (BX_3) system exhibits a pronounced downfield shift with respect to upfield ^{11}B signals for BX_4^-.

In order to expand ^{11}B NMR structural studies in the series of compounds with one boron atom only and with subsequent analyses of the computed shielding tensors, we carried out ^{11}B NMR shifts calculations for BX_3 /BX_4^- pairs with a greater variety of X, i.e. for X = H, CH_3, F, Cl, Br, I, OH, SH, NH_2, and CH=CH_2. The fact that detailed analyses of the shielding tensors are missing in refs.10 and 11 we included halogens in this study, too. We also refined the geometries at a higher level (RMP2(fc)) than was done in most previous studies and took scalar and spin-orbit relativistic effects into account. The sophisticated statistical method, known as the factor analysis, was applied for assessing NMR substitution effects, since this approach frequently used in chemometrics is mainly intended for giving physical meaning of the factors obtained.

■ RESULTS AND DISCUSSION

At first, the geometries were optimized at the RMP2(fc)/6-31+G** level of theory within the given symmetry restrictions, see Fig.1.

BX_3.The molecular geometries of BX_3 can be compared with gas-phase experimental internal coordinates (Table 1), where available. In general there is a very good agreement between the computed B-X distances and those determined in the gas phase.
These systems have three electron pairs in the valence shell of the B atom, and in light of the valence-shell electron pair repulsion (VSEPR[22]) approach trihalogenated boron arrangements are planar. Most BX_3 structures of this study are strictly planar possessing D_{3h} or C_{3h} symmetry, except for X = NH_2 and CH=CH_2, which adopt C_s and C_3 symmetric structures, respectively. Even in these cases, where a plane of symmetry through the BX_3 moiety is absent, the B atoms are essentially planar (the angle sums at B are very close to 360°). An

interesting feature was found in the electron-diffraction study of $B(CH=CH_2)_3$;[23] the slight elongation of the C=C bond length in the electron-diffraction structure, 1.370(6) Å , (cf. 1.353 Å at the RMP2(fc)//6-31+G** level) with respect to a standard C=C double bond was asribed to p(π)-donation between the C=C double bond and the vacant $2p_z$ orbital on the B atom.

Computed ^{11}B chemical shifts are collected in Table 3 and are compared to previous theoretical and experimental data from the literature. It is clearly seen that ^{11}B nucleus in almost all BX_3 compounds resonates at higher frequencies (i.e. is more shielded than in BH_3), X=I represents the most notable exception, mainly due to large contribution of the SO coupling to the shielding of BI_3. The most deshielded ^{11}B resonance is found for X = CH_3, which is in accord with the very large anisotropy of ^{11}B. The latter is comparable with that in BH_3, which is computed to be the largest one in the whole series. The nonrelativistic GIAO-anisotropy values (without considering SO coupling) increases in the order of OH ‹ F ‹ NH_2 ‹ Cl ‹ Br $CH=CH_2$ ‹ I ‹ SH ‹ CH_3 ‹ H (Table 3), which roughly corresponds to the opposite trend of the p(π)- donation abilities of X.[24,25] When X does not possess a free electron pair, the $2p_z$ orbital on B remains unoccupied, which results in deshielding of this atom and, consequently, a large shift to high frequency is observed. This is particularly true for X = H, CH_3. BH_3 has a very low-lying LUMO orbital (0.056a.u. at HF/II, II stands for a Huzinaga-type basis set developed for NMR computations, for further applications see ref. 2a,b), which is responsible for the strongly deshielding contributions from the BH bonds. Replacement of H with CH_3 changes this situation very little. The deshielding by a BF bond in BF_3, for example, is roughly six times smaller than that of a BH bond in BH_3. Furthermore, the occupancy in the $2p_z$ orbital of the B atom for $B(NH_2)_3$ is 0.491 as found in terms of the NBO analysis, which is the highest value in this series.[26] The $2p_z$ occupancies of the other BX_3 systems are collected in Table 4. The C_s structure of $B(NH_2)_3$ (a true minimum on the corresponding PES, the D_{3h} structure is a saddle point of the first order) revealed geometrical consequences of the p(π)-back donation in terms of two different BN bond lengths. By going to the hypothetical D_{3h} structure of this compound (with all H atoms out of plane, NIMAG = 2 at MP2/6-31+G*), this p(z)-p(π) interaction is all but shut off (the $2p_z$ occupancy amounts to just 0.069 from weak hyperconjugation of the NH bonds). As a consequence, the calculated δ(^{11}B) value is 47.3 ppm; the p(z)-p(π) interaction in the C_s minimum thus produces a shielding of the ^{11}B resonance of more than 20 ppm.

B(OH)$_3$ and B(SH)$_3$ behave in the same manner (for the C_{3v} structures with out-of-plane H atoms NIMAG = 3) but due to two lone electron pairs on oxygen and sulphur p(π)-donation remains virtually unchanged in the various stationary points, with little influence on the δ(^{11}B) values.

Interestingly, ^{11}B in a hypothetical B(CN)$_3$ resonates at 27.1 ppm (GIAO-MP2/II//MP2/6-31+G**), which is a value very similar to that found for ^{11}B in B(NH$_2$)$_3$, even though the cyano group is usually regarded to be electron acceptor in contrast to the electron-donating ability of NH_2. Apparently there is enough π-donation from the cyano groups to inrease the ^{11}B shielding from that in the truly electron-deficient BH_3. The boron atom in the quite recently prepared B(CN)$_3^{2-}$ with nucleophilic abilities[27] of this boron resonates at -45.3 ppm (in ND_3, -51.9 ppm for GIAO-MP2/II//MP2/6-31+G**). This strong shielding is in part due to the more negatively charged boron than in B(CN)$_3$, but mostly because of the unavailabiliy of low-lying unoccupied orbitals in the reduced form with its formal octet at boron.

BX_4^-. The molecular geometrical parameters of BX_4^- are collected in Table 2. The additional substituents in the OH, SH, NH_2 and CH=CH$_2$ groups lead to a reduction in symmetry from T_d to S_4 (or to D_{2d}, but the latter structures turned out to be higher in energy and were not considered further). In the optimised minima, some noticeable deviations of the XBX bond angles from the ideal tetrahedral angle were observed. These deviations were rationalised on the basis of a detailed analysis of calculated electron density distributions by employing atom-in-molecule approach.[28] Fig. 2 clearly shows the asymmetry of the electron density distribution, consistent with the so-called ligand-close packing model (LCP).[29,30] The S_4 geometries are in overall agreement with experimentally determined ones and were utilized in NMR shift calculations. Computed and experimental $\delta(^{11}B)$ data agree very well (see Table 3). We note in passing that for the systems with the lighter substituents the non-relativistic MP2 method performs somewhat better than ZORA-SO-BP86 (which is very close to NREL-BP86 in these cases), but for the heavier substituents, where spin-orbit coupling becomes important, ZORA-SO-BP86 is clearly superior.The ^{11}B anisotropies are zero by symmetry for T_d structures or almost zero for S_4 minima. Because no low-lying virtual orbitals are present, paramagnetic contributions[31] are significantly reduced and the B atoms in BX_4^- resonate at lower frequencies than those in BX_3.[32]

Attempts were made to apply linear regression between the ^{11}B shieldings in the BX_3 series (either the isotropic averages σ_{iso} or individual principal components σ_{ii}) and other computed variables such as orbital occupancies or inverse energy differences $1/\Delta E$ between suitable occupied and unoccupied MOs (mostly HOMO and LUMO)[33] and inductive prameters σ_I by Taft.[34] No simple correlations were found and, therefore, factor analysis [35,36] has been applied to a data matrix formed by 7 variables for all X (see Table 4). Basically, these variables comprise the constituents of the Ramsey equation with the exception of the Taft constants ,charges based on natural population analysis (NPA), and magnitude (V_{max}) of the so-called π-hole[37] on the respective boron atom (see Fig. 3).[38-40] V_{max} is defined as the value of the most positive electrostatic potential of an electron density surface. This procedure involves, in its last steps, a solution of a secular problem that consists of the diagonalization of the correlation matrix (see Table 5) As a result, it turns out that three factors comprise 92 % of the cumulative proportion of the total variance (for the factor values in terms of the original descriptors, see Table 6). The main components of the first factor (45 % proportion of the total variance) are occupancies in the p_x and p_y orbitals and $1/\Delta E$ (inverse energy difference between suitable occupied and unoccupied MOs), the second factor (26 % proportion of the total variance) is mainly the occupancy in the p_z orbital and the inductive substituent parameters by Taft and the third factor (21 % proportion of the total variance) consists exclusively (99.3 %) of the maximum values of the electrostatic potentials (V_{max}), i.e. π-hole magnitudes. When both shielding descriptors (i.e. σ_z and $(\sigma_{xx} + \sigma_{yy})/2$) were added to the statistical computation, the newly obtained three factors predicted 94 % of the variance and they were composed similarly as if 7 descriptors only were allowed to be statistically treated. Note that although a nine-descriptor model accounts for in terms of five factors 98 % of the cumulative proportion of the total variance, it is not physically correct since for the axially symmetric BX_3 systems the isotropic shielding is fully described by these two extra descriptors (when having a large statistical set of data, they should describe 100 % of the total variance).

Computational details

Molecular geometries were optimized with the given symmetry restrictions at the HF/6-31+G** and RMP2(fc)/6-31+G** levels, using relativistically adjusted pseudopotentials on Br and I along with corresponding valence basis sets of polarized double-zeta quality.[41] Second derivative analyses were carried out at the HF/6-31+G** level to verify the minimum character of the stationary points. These computations were run with Gaussian 09.[42] Electrostatic potentials were computed at HF/ 6-31+G** level using Gaussian09 and Molekel4.3[43,44] programs.

Magnetic shieldings were calculated using the GIAO-MP2 method[45-47] that are incorporated into the Gaussian 09 suite of programs. The IGLO-II basis se[48] was used throughout for S, B, C, N, F, Cl, Br, I and H, respectively,

Additional NMR calculations were performed with the Amsterdam density functional (ADF) code employing the BP86 functional.[49,50] The two-component relativistic zeroth-order regular approximation (ZORA) method[51-53] including scalar and spin-orbit (SO)[54] corrections was employed for these computations. ADF scheme was also used without SO corrections with the same BP86 functional. ^{11}B chemical shifts were calculated relative to B_2H_6 and converted to the usual $BF_3{\cdot}OEt_2$ scale using the experimental $\delta(^{11}B)$ value for B_2H_6 of 16.6 ppm.[24] NMR chemical shifts are given in Table 2. Statistical analyses were carried out with the *R* software[55]

■ CONCLUSIONS

There is a very good accord between the computed and experimentally determined ^{11}B chemical shifts in monoboranes BX_3 and BX_4^-. When X is a light element from the first and second periods, spin-orbit contributions to the magnetic shieldings are small, and both GIAO-MP2 and NREL/BP86 perform almost equally well. In contrast, for the heavier halogens, i. e. for X = Br and in particular for X = I, spin-orbit contributions are dominant, and a corresponding relativistic treatment is mandatory.

For the BX_3 species with their essentially trigonal planar boron center, the highest nuclear shielding component is the one perpendicular to the plane (σ_{zz}) , and the strongest deshielding (σ_{xx} and σ_{yy}) is found along axes in the plane. This deshielding arises from magnetic couplings between the occupied B-X bonding orbitals and the unoccupied p-orbital on B

The ^{11}B shielding of the boron atoms in both BX_3 and BX_4^- series depends on various variables, which was proved for the trigonal compounds in terms of applying factor analysis

The overall shielding of ^{11}B is the result of counteracting influences, which may affect the individual tensor components differently, thus affecting the anisotropy. The $\delta(BX_3)$ - $\delta(BX_4^-)$ difference nicely reflects the strength of p(π)-back donation abilities of X since other factors are largely kept constant. The most pronounced difference in the $\delta(^{11}B)$ values is found for BI_3 and BI_4^-, which can be ascribed to the additive character of the spin-orbit contributions from the B-I bonds. The BBr_3 and BBr_4^- pair behaves similarly.

No simple correlations between computed shieldings and single descriptors could be found, but factor analysis revealed that the variance in the shieldings can be well described by a small group of descriptors, mainly consisting of the p-orbital occupations, energy differences between suitable occupied and unoccupied orbitals, as well as inductive substituent parameters and maximum values of the electrostatic potentials, i.e. magnitudes of the π-holes.

■ ACKNOWLEDGMENTS

The financial support of the Czech Science Foundation (project No. 17-08045S) is gratefully acknowledged.

■ REFERENCES

1 Lipscomb, W.N. *Boron Hydrides*, Benjamin, New York, 1963.

2 Hnyk, D.; Wann, D.A. *Boron – the Fifth Element,* Chapter 2, Molecular Structure of Free Boron Clusters. In *Challenges and Advances in Computational Chemistry and Physics.* Vol 20, Hnyk, D.; McKee, M., Eds., Springer, Heidelberg, New York, Dordrecht and London, 2015.

3 Hnyk, D.; Rankin, D. W.H. Stereochemistry of Free Boranes and Heteroboranes from Electron Scattering and Model Chemistries. *Dalton Trans.* **2009,** 585 - 599.

4 Mastryukov, V.S. Boron and Silicon Compounds. In *Stereochemical Applications of Gas Phase Electron Diffraction*; Hargittai, I.; Hargittai, M., Eds.; VCH: New York, 1998; Part B, 1-34.

5 There are four spin functions of ^{11}B, function (total spin): A (+3/2) ααα, B(+1/2) $1/\sqrt{3}(\alpha\alpha\beta + \alpha\beta\alpha + \beta\alpha\alpha)$, Γ(-1/2) $1/\sqrt{3}(\alpha\beta\beta + \beta\alpha\beta + \beta\beta\alpha)$, Δ (-3/2) βββ. The individual components of the spin operator work as follows: $S_xA = \sqrt{3}/2B$, $S_xB = \Gamma+\sqrt{3}/2A$, $S_x \Gamma = B + \sqrt{3}/2\ \Gamma$, $S_x \Delta = \sqrt{3}/2\ \Delta$; $S_yA = i\sqrt{3}/2B$, $S_yB = iC - i\sqrt{3}/2B$, $S_y \Gamma = iB + i\sqrt{3}/2\Delta$, $S_y \Delta = -i\sqrt{3}/2\ \Gamma$; $S_zA = 3/2A$, $S_zB = 1/2B$, $S_z \Gamma = -1/2\Gamma$, $S_z \Delta = -3/2\Delta$.

6 Hnyk, D.; Jayasree, E.G. Cationic *Closo*-Carboranes 2. Do ^{11}B and ^{13}C NMR Chemical Shifts Support Their Experimental Availability? *J. Comput. Chem.* **2013**, *34*, 656 - 661 and references therein.

7 Štíbr, B.; Tok, O. L; Holub, J. Quantitative Assessment of Substitution NMR Effects in the Model Series of *o*-Carborane Derivatives: α-Shift Correlation Method. *Inorg. Chem.* **2017**, *56*, 8334-8340.

8 Štíbr, B. ^{11}B-NMR Shielding Effects in the *Closo* Borane Series. Sensitivity of Shifts and their Additivity. *New. J. Chem.* **2017**, DOI: 10.1039/C7NJ02689G.

9 Two-determinant numerical self-consistent atomic orbitals for ^{11}B itself were determined, see Spagnolo, F.A.; Burke, E.A. Two-Determinant Numerical Self-Consistent Atomic Orbitals: Application to ^{11}B. *J. Chem. Phys.* **1979**, *71*, 750 - 754.

10 Kaupp, M. Relativistic Effects on NMR Chemical Shifts. In *Relativistic Electronic Structure Theory II: Applications*, P. Schwerdtfeger, ed., Elsevier, Amsterdam, **2004**.

11 Mercier, H.P.A.; Moran, M.D.; Schrobilgen, G.J.; Steinberg, Ch.; Suontamo, R.J. The Syntheses of Carbocations by Use of the Noble-Gas Oxidant, $[XeOTeF_5][Sb(OTeF_5)_6]$: The Syntheses and Characterization of the CX_3^+ (X = Cl, Br, $OTeF_5$) and $CBr(OTeF_5)_2^+$ Cations and Theoretical Studies of CX_3^+ and BX_3 (X = F, Cl, Br, I, $OTeF_5$). *J. Am. Chem. Soc.* **2004**, *126*, 5533 – 5548.

12 Interestingly, a very good agreement with the experimental values was achieved by using multidimensional regression analysis based on higher degree polynomials, well-established for predictive purposes: Nanney, J.R.; Jetton, R.E.; Mahaffy, C.A.L. The Prediction of the ^{11}B Signal Positions of Trigonal Boranes Using Statistical Methods. *Electronic Journal of Theoretical Chemistry*. **1997**, *2*, 24 - 48.

13 Kaupp,M; Malkina, O.L.; Malkin, V. G. Interpretation of ^{13}C NMR Chemical Shifts in Halomethyl Cations. On the Importance of Spin-Orbit Coupling and Electron Correlation. *Chem. Phys. Lett.* **1997**, *265*, 55 - 59.

14 Kaupp, M.; Malkina, O.L.; Malkin, V.G.; Pyykkö, P. How Do Spin–Orbit-Induced Heavy-Atom Effects on NMR Chemical Shifts Function? Validation of a Simple Analogy to Spin–Spin Coupling by Density Functional Theory (DFT) Calculations on Some Iodo Compounds. *Chem. Eur. J.*, **1998**, ***4***, 118 - 126.

15 Ramsay, N.F. Magnetic Shielding of Nuclei in Molecules. *Phys. Rev.* **1950**, *78*, 699.

16 The Ramsey equation was modified by Pople, see Pople, J.A. The Theory of Carbon Chemical Shifts in N.M.R. *Mol. Phys.* **1964**, *7*, 301 - 306.

17 Saika, A.; Schlichter, C.P. *J. Chem. Phys.* **1954**, *22*, 26.

18 Wiberg, K.B.;Hammer, J. D. ; Keith, T.A.; Zilm, K. *J. Phys. Chem A* **1999**, *103*, 21.

19 See also the resulting "orbital rotation model": Autschbach, J.; Zheng, S. Analyzing Pt Chemical Shifts Calculated from Relativistic Density Functional Theory Using Localized Orbitals: The Role of Pt 5d Lone Pairs. *Magn. Reson. Chem*. **2008**, 46, S45-S55.

20 Hartman, J.S.; Schrobilgen, G.J. Mixed Tetrahaloborate Ions. Detection and Study by Nuclear Magnetic Resonance. *Inorg. Chem*. **1972**, *11*, 940 - 951.

21 Heřmánek, S. Boron-11 NMR Spectra of Boranes, Main-Group Heteroboranes, and Substituted Derivatives. Factors Influencing Chemical Shifts of Skeletal Atoms. *Chem. Rev.* **1992**, *92*, 325 - 362: H, CH_3, OH, SH, NH_2, and $CH=CH_2$ can also coordinate boron atom in the both structural motifs.

22 Gillespie, R.J. *Molecular Geometry,* Van Nostrand Reinhold, London, 1972.

23 Foord, A.; Beagley, B.; Reader, W.; I. Steer, I.A. A Gas-Phase Electron-Diffraction Study of Trivinylborane. *J. Mol. Struct.* **1975**, *24*, 131-137.

24 Onak, T.; Landesman, H.; Williams, R.E.; Shapiro, I. The B^{11} Nuclear Magnetic Resonance Chemical Shifts and Spin Coupling Values for Various Compounds. *J. Phys. Chem.* **1959**, *63*, 1533 - 1535.

25 Good, C.D.; Ritter, D.M. Alkenylboranes. II. Improved Preparative Methods and New Observations on Methylvinylboranes. *J. Am. Chem. Soc.* **1962**, *84*, 1162 - 1166.

26 Reed, A.E.; Weinstock, R.B.; Weinhold, F. Natural Population Analysis. *J. Chem. Phys.* **1985**, *83*, 735 - 746.

27 Bernhardt, E.; Bernhardt – Pitchougina, V.; Willner, H.; Ignatiev, N. "Umpolung" at Boron by Reduction of $[B(CN)_4]^-$ and Formation of the Dianion $[B(CN)_3]^{2-}$.*Angew. Chem. Int. Ed.* **2011**, *50*, 12085 - 12088.

28 Bader, R.F.W. *Atoms in Molecules* Oxford Press, New York, 1990.

29 Robinson, E.A.; Johnson, S.A.; Tang, T.H.; Gillespie, R.J. Reinterpretation of the Lengths of Bonds to Fluorine in Terms of an Almost Ionic Model. *Inorg. Chem.* **1997**, *36*, 3022 - 3030 and references therein.

30 Alder, R.W.; Allen, P.R.; Hnyk, D.; Rankin, D.W.H.; Robertson, H.E.; Smart, B.A.; Gillespie, R.J.; Bytheway, I.A. Molecular Structure of 3,3-Diethylpentane (Tetraethylmethane) in the Gas Phase As Determined by Electron Diffraction and ab Initio Calculations. *J. Org. Chem.* **1999**, *64*, 4226 - 4232.

31 In effect, paramagnetic contributions only vanish in atoms; e.g. a hypothetical B^+ ($1s^2$ $2s^2$ configuration) has a much higher shielding than e.g. BH_4^-.

32 In the classical Ramsey expression not only the energy gap between occupied and virtual orbitals enters (by way of the mean excitation energy), but also the mean expectation value of the inverse cube of the 2p orbital radius; as the bond lengths contract on going from BX_4^- to BX_3 (see Tables 1,2), this factor is expected to increase, leading to more negative paramagnetic contribution to the overal shielding of boron and, in turn, to downfiled ^{11}B chemical shift.

33 To be coupled magnetically, occupied and unoccupied MOs must have different symmetries. For instance, a magnetic (angular momentum) operator in the molecular plane couples an occupied orbital with p_x or p_y contribution on B with an unoccupied MO with p_z contribution on B. In the planar BX_3 species, the p_z orbital is usually very prominent in the LUMO; the suitable occupied MOs to couple with it were chosen as the highest ones that contain p_x or p_y cotributions on B. These are mostly (but not always) the HOMOs.

34 E.g. Taft, R. W.; Lewis, I.C. The General Applicability of a Fixed Scale of Inductive Effects. II. Inductive Effects of Dipolar Substituents in the Reactivities of m- and p-Substituted Derivatives of Benzene. *J. Am. Chem. Soc.* **1958**, *80*, 2436 - 2443.

35 For the general overview see e.g. Harman, H.H.; *Modern Factor Analysis* University Chicago Press, Chicago 1970.

36 For a chemical application see e.g. Hnyk, D. Principal Component Analysis of Substituent Constants. *Collect. Czech. Chem. Commun.* **1990**, *55*, 55 - 62 and references therein

37 Wang, H.; Wang, W.; Jin, W.J. σ-Hole Bond vs π-Hole Bond: A Comparison Based on Halogen Bond. *Chem. Rev.* **2016**, *116*, 5072 - 5104.

38 Fanfrlík, J.; Švec, P.; Růžičková, Z.; Hnyk, D.; Růžička, A.; Hobza, P. The Interplay between Various σ- and π-Hole Interactions of Trigonal Boron and Trigonal Pyramidal Arsenic Triiodides. *Crystals* **2017**, *7*, 225.

39 Note that π-holes in various ZX_3 Lewis bases are responsible for their interactions with nitrogen compounds, see Grabowski, S.J. Boron and other Triel Lewis Acid Centers: From Hypovalency to Hypervalency. *ChemPhysChem* **2014**, *15*, 2985-2993.

40 Grabowski, S.J. π-Hole Bonds: Boron and Aluminum Lewis Acid Centers. *ChemPhysChem* **2015**, *16*, 1470 - 1479.

41 Bergner, A.; Dolg, M.; Küchle, W.; Stoll, H.; Preuss, H. *Ab initio* Energy-adjusted Pseudopotentials for Elements of Groups 13–17. *Mol. Phys.* **1993**, *80*, 1431 -1441.

42 Frisch, M. J.; Trucks, G. W.; Schlegel, H. B.; Scuseria, G. E.; Robb, M. A.; Cheeseman, J. R.; Scalmani, G.; Barone, V.; Mennucci, B.; Petersson, G. A.; Nakatsuji, H.; Caricato, M.; Li, X.; Hratchian, H. P.; Izmaylov, A. F.; Bloino, J.; Zheng, G.; Sonnenberg, J. L.; Hada, M.; Ehara, M.; Toyota, K.; Fukuda, R.; Hasegawa, J.; Ishida, M.; Nakajima, T.; Honda, Y.; Kitao, O.; Nakai, H.; Vreven, T.; Montgomery, Jr., J. A.; Peralta, J. E.; Ogliaro, F.; Bearpark, M.; Heyd, J. J.; Brothers, E.; Kudin, K. N.; Staroverov, V. N.; Kobayashi, R.; Normand, J.; Raghavachari, K.; Rendell, A.; Burant, J. C.; Iyengar, S. S.; Tomasi, J.; Cossi, M.; Rega, N.; Millam, J. M.; Klene, M.; Knox, J. E.; Cross, J. B.;

Bakken, V.; Adamo, C.; Jaramillo, J.; Gomperts, R.; Stratmann, R. E.; Yazyev, O.; Austin, A. J.; Cammi, R.; Pomelli, C.; Ochterski, J. W.; Martin, R. L.; Morokuma, K.; Zakrzewski, V. G.; Voth, G. A.; Salvador, P.; Dannenberg, J. J.; Dapprich, S.; Daniels, A. D.; Farkas, Ö.; Foresman, J. B.; Ortiz, J. V.; Cioslowski, J.; Fox, D. J. *Gaussian 09, Revision D.1*, Gaussian, Inc., Wallingford CT, 2009.

43 MOLEKEL 4.3, Flűkiger, P.; Lűthi, H.P.; Portmann, S.; Weber J. *Swiss Center for Scientific Computing*, Manno (Switzerland), 2000.

44 Portmann, S.; Luthi, H.P. MOLEKEL: An Interactive Molecular Graphic Tool. *CHIMIA Int. J. Chem.* **2000**, *54*, 766 - 770.

45 Ditchfield, R. Self-consistent perturbation theory of diamagnetism. *Mol. Phys.* **1974**, *27*, 789 - 807.

46 Wolinski, K.; Hinton, J.F.; Pulay, P. Efficient implementation of the gauge-independent atomic orbital method for NMR chemical shift calculations. *J. Am. Chem. Soc.* **1990**, *112*, 8251 - 8260.

47 Gauss, J. Effects of Electron Correlation in the Calculation of Nuclear Magnetic Resonance Chemical Shifts. *J. Chem. Phys.* **1993**, *99*, 3629.

48 Kutzelnigg, W.; Fleischer, U.; Schindler, M. *NMR Basic Principles and Progress*, Springer, Berlin, 1990, *23*, 165.

49 Becke, A.D. Density-Functional Exchange-Energy Approximation with Correct Asymptotic Behavior. *Phys. Rev. A* **1988**, *38*, 3098 - 3100.

50 Perdew, J.P. Density-Functional Approximation for the Correlation Energy of the Inhomogeneous Electron Gas. *Phys. Rev. B* **1986**, *33*, 8822 - 8824.

51 van Lenthe; E.; Baerends, E. J.; Snijders, J. G. Relativistic Total Energy Using Regular Approximations. *J. Chem. Phys.* **1994**, *101*, 9783.

52 van Lenthe, E.; van Leeuwen, R.; Baerends, E. J.; Snijders, J. G. Relativistic Regular

Two-Component Hamiltonians. *Int. J. Quantum Chem.* **1996**, *57*, 281 – 293.

53 van Lenthe, E.; Baerends, E. J.; Snijders, J. G. Relativistic Regular Two-Component Hamiltonians. *J. Chem. Phys.* **1993**, *99*, 4597.

54 van Lenthe, E.; Snijders, J. G.; Baerends, E. J. The Zero-Order Regular Approximation for Relativistic Effects: The Effect of Spin–Orbit Coupling in Closed Shell Molecules. *J. Chem. Phys.* **1996**, *105*, 6505.

55 R Core Team, *R: A Language and Environment for Statistical Computing*, https://www.R-project.org, R Foundation for Statistical Computing, Vienna, 2016

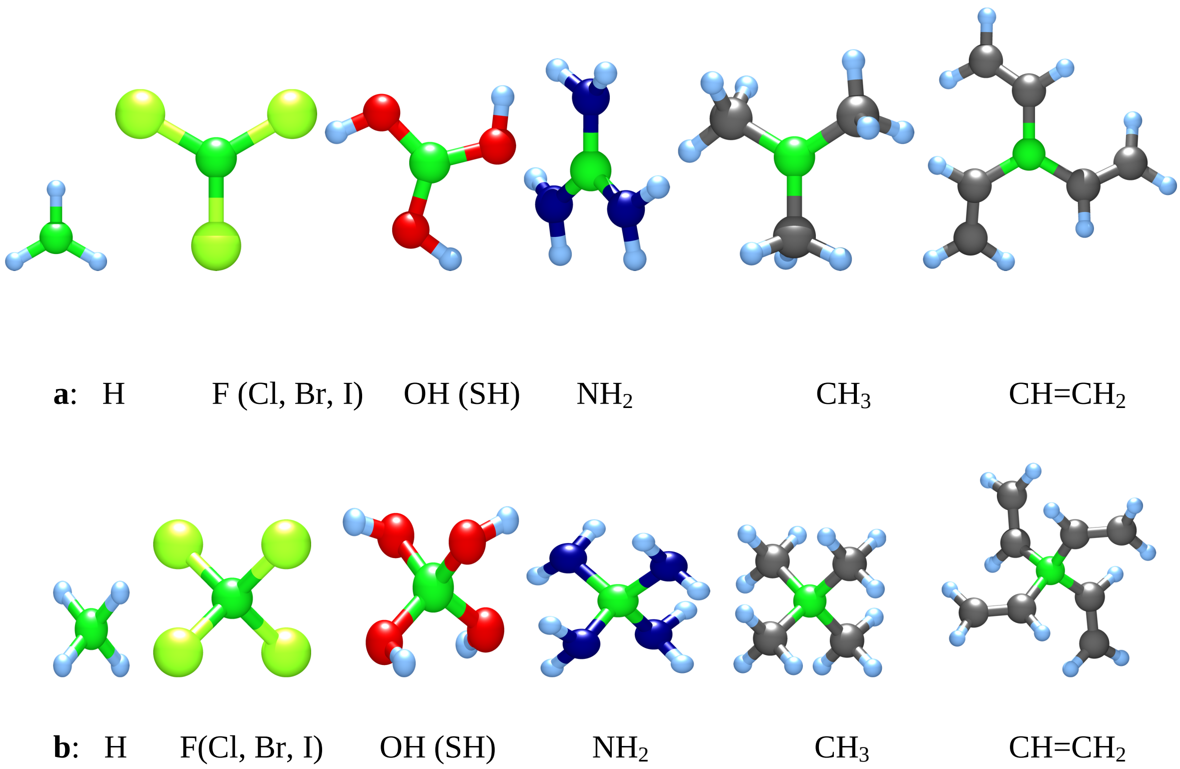

Fig. 1 Molecular diagrams of a) BX_3 and b) BX_4^- in the corresponding symmetries

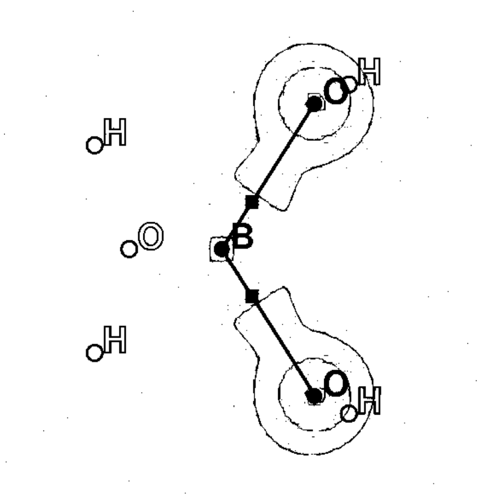

B(OH)$_4^-$: ρ = 0.156, $\nabla^2\rho$ = 0.646

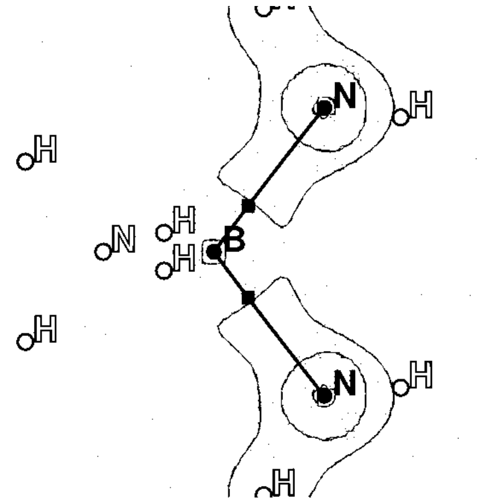

B(NH$_2$)$_4^-$: ρ = 0.150, $\nabla^2\rho$ = 0.338

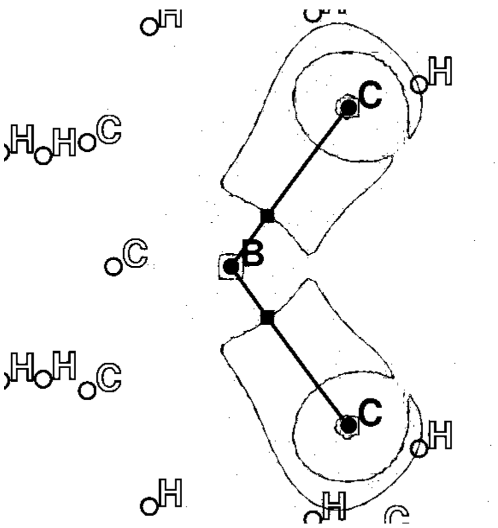

B(CH=CH$_2$)$_4^-$: ρ = 0.152, $\nabla^2\rho$ = 0.094

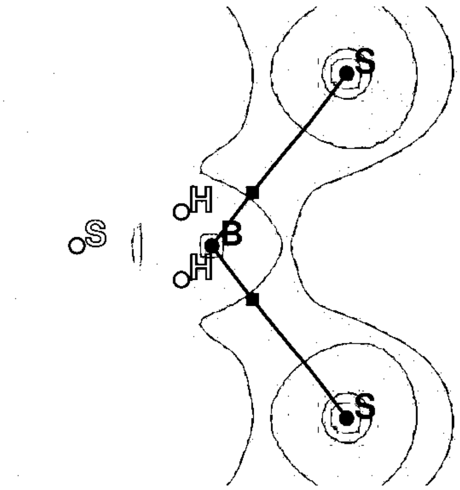

B(SH)$_4^-$: ρ = 0.125, $\nabla^2\rho$ = -0.212

Fig.2 RMP2/6-31+G** AIM results for S_4-symmetrical BX_4^-, electron density (ρ) and its Laplacian ($\nabla^2\rho$) are in a.u.

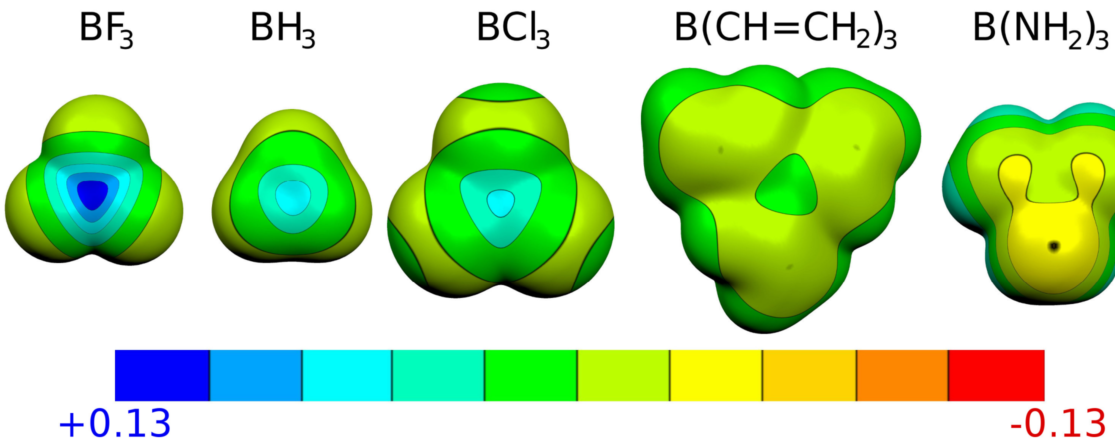

Fig. 3 The computed electrostatic potentials (ESP) on a 0.001 a.u. molecular surface of the selected BX_3 systems with the most striking ESP values, for their real values see Table 6. The colour range of the ESP in a.u. Note that BH_3 has more positive π-hole than BCl_3

Table 1 Ab Initio Optimized B-X Bond Lenghts for BX_3 Systems (in Å, X= H, F, Cl, Br, I, $C(_{sp}{}^{3})$-H_3, N, O, S, $C(_{sp}{}^{2})H{=}CH_2$)

		r(B-X)	
Compound	Symmetry	RMP2(fc)//6-31+G**	electron diffraction[a]
BH_3	D_{3h}	1.186	—
BF_3	D_{3h}	1.328	1.313(1)
BCl_3	D_{3h}	1.738	1.742(4)
BBr_3	D_{3h}	1.902	1.893(5)
BI_3	D_{3h}	2.135	2.118(5)
$B(CH_3)_3$	C_{3h}	1.577	1.578(1)
$B(NH_2)_3$	C_s	2 ×1.436 + 1 × 1.439	1.432(2)[b]
$B(OH)_3$	C_{3h}	1.377	1.368(2)[c]
$B(SH)_3$	C_{3h}	1.806	1.805(2)[d]
$B(CH{=}CH_2)_3$[c]	C_3[c]	1.561	1.558(3)

[a]Ref 4. [b]$NHCH_3$. [c]OCH_3. [d]SCH_3.

Table 2 Salient Ab Initio Optimized (RMP2(fc)//6-31+G** Level) Structural Parameters or some BX_4^- Systems (X=X= H, F, Cl, Br, I, $C(_{sp}{}^3)$-H_3, N, O, S, $C(_{sp}{}^2)H=CH_2$)

Compound	Symmetry	r(B-X)	∠ XBX	∠ XBX	τ (X-B-X...X)
BH_4^-	T_d	1.233	6 × 109.5		4 × [2 × 120 + (2 × -120)]
BF_4^-	T_d	1.423	6 × 109.5		4 × [2 × 120 + (2 × -120)]
BCl_4^-	T_d	1.857	6 × 109.5		4 × [2 × 120 + (2 × -120)]
BBr_4^-	T_d	2.030	6 × 109.5		4 × [2 × 120 + (2 × -120)]
BI_4^-	T_d	2.277	6 × 109.5		4 × [2 × 120 + (2 × -120)]
$B(CH_3)_4^-$	T_d	1.647	6 × 109.5		4 × [2 × 120 + (2 × -120)]
$B(NH_2)_4^{-\,a}$	S_4	1.560	2 × 104.2	4 × 112.2	4 × [± 121.6 + (± 116.9)]
$B(OH)_4^{-\,b}$	S_4	1.490	2 × 115.4	4 × 106.6	4 × [± 118.1 + (± 123.8)]
$B(SH)_4^{-\,c}$	S_4	1.928	2 × 102.9	4 × 112.9	4 × [± 121.9 + (± 116.1)]
$B(CH=CH_2)_4^{-\,d}$	S_4	1.621	2 × 106.6	4 × 110.9	4 × [± 120.9 + (± 118.3)]

[a,b,c,d] The corresponding D_{2d} forms are disfavored with respect to the S_4 forms by 67.4, 32.4, 28,4 and 73.5 kcal.mol^{-1}, resp.

Table 3 Computed overall ^{11}B NMR chemical shifts[a], anisotropies, and σ_{zz} components of the shielding tensors

					BX_3					
					X					
X	H	F	Cl	Br	I	CH_3	$CH=CH_2$	OH	NH_2	SH
NR-B3LYP/cc-pVTZ[b]		24.0	68.8	73.1	117.8					
SSCS[c]		10.4	46.6	43.7		84.4	59.3	16.5	23.9	62.5
NR-MP2/II[d,e]	87.4	13.2	51.4	73.1	102.8	90.3	56.1	22.0	26.0	62.7
^{11}B anisotropy $\Delta\sigma$[f]	184.4	8.9	35.5	61.5	111.8	153.8	94.8	5.3	37.6	118.7
σ_{zz}	148.9	88.4	85.7	81.4	85.2	125.7	120.5	94.9	75.0	102.0
BP86/QZ4P [g,h]	94.5	7.3	48.2	68.7	95.6	89.4	47.1	16.3	18.9	57.7
ZORA-SO-BP86/Q4Z[g,i]	94.6	7.2	43.4	37.9	-5.2	89.4	47.3	16.2	18.8	55.2
SO coupling[g,i]	0.4	0.9	5.5	32.6	105.8	0.5	0.3	0.6	0.5	3.2
Experimental[f]	*70.0*	*10.0*	*46.5*	*38.7*	*-7.9*	*86.2*	*56.4*	*18.8*	*24.6*	*61.6*
					$[BX_4]^-$					
					X					
X	H	F	Cl	Br	I	CH_3	$CH=CH_2$	OH	NH_2	SH
NR-MP2/II[d]	-46.9	1.0	13.5	15.6	25.0	-19.3	-12.8	3.4	0.4	4.5
^{11}B anisotropy $\Delta\sigma$[f]	0	0	0	0	0	0	0.1	7.4	5.6	12.0
σ_{zz}	160.3	112.4	99.9	90.8	88.5	132.7	126.3	114.9	105.5	92.9
BP86/QZ4P[g,h]	-40.0	-2.4	13.2	22.4	21.4	-30.0	-19.8	-1.9	-7.6	1.2
ZORA-SO-BP86//QZ4P[g,i]	-60.5	-3.6	5.7	-25.2	-136.1	-30.0	-19.7	-2.1	-7.7	-3.5
SO coupling[g,i]	0.4	1.2	8.5	51.2	168.8	0.5	0.4	0.8	0.6	5.7
Experimental[j]	*-40.0*	*-1.6*	*6.7*	*-23.8*	*-127.5*	*-20.2*	*-16.1*	*1.1*	*0.2*	*6.3*

[a]With respect to $BF_3.OEt_2$. [b]Ref. 11 (nonrelativistic GIAO level), [c]Statistical substituent chemical shift, see Ref. 12. [d]This work at GIAO nonrelativistic level. [e]Gaussian 09. [f] Defined as $\Delta\sigma = \sigma_{zz} - (\sigma_{xx} + \sigma_{yy})/2$ and reported as computed in this work. [g]ADF, this work. [h]Scalar relativistic level, this work [i] SO coupling based on ZORA-SO/QZ4P. [j]Ref. 21.

Table 4 Data matrix used in the factor analysis[a]

	p_z	$(p_x + p_y)/2$	$1/\Delta E$	NPA	σ_I (Taft)	r(B-X)	V_{max}
H	0.000	0.815	1.802	0.38	0.00	1.186	0.073
F	0.242	0.364	1.186	1.68	0.54	1.328	0.125
Cl	0.393	0.675	1.739	0.44	0.47	1.738	0.057
Br	0.420	0.754	2.012	0.10	0.47	1.902	0.052
I	0.466	0.846	2.433	-0.33	0.40	2.135	0.041
CH_3	0.110	0.636	1.757	1.00	-0.01	1.577	0.046
$CH{=}CH_2$	0.217	0.674	1.980	0.82	0.12[b]	1.561	0.019
OH	0.312	0.433	1.397	1.45	0.24	1.377	0.041
SH	0.473	0.787	1.730	0.06	0.27	1.806	0.013
NH_2	0.533	0.450	1.613	1.07	0.17	1.437	-0.135

[a]For the meaning of the descriptors see the text (orbital occupations and Taft parameters dimensionless, ΔE in eV, distances in Å, V_{max} in a.u.). [b]Benzene value

Table 5 Correlation matrix among the individual descriptors

	p_z	$(p_x + p_y)/2$	$1/\Delta E$	NPA	σ_I (Taft)	r(B-X)	V_{max}
p_z	1	-0.03489489	0.1852445	-0.30375825	0.5575341	0.61805243	-0.5331977
$(p_x + p_y)/2$	-0.03489489	1	0.8307477	-0.93411149	-0.1430914	0.57414978	0.12656124
$1/\Delta E$	0.18524447	0.83074771	1	-0.85364542	-0.0640016	0.73968121	-0.10812155
NPA	-0.30375825	-0.93411149	-0.8536454	1	-0.1017752	-0.7516777	0.02681515
σ_I (Taft)	0.55753411	-0.14309142	-0.0640016	-0.1017752	1	0.44498695	0.32460697
r(B-X)	0.61805243	0.57414978	0.7396812	-0.7516777	0.4449869	1	-0.03737448
V_{max}	-0.5331977	0.12656124	-0.1081216	0.02681515	0.324607	-0.03737448	1

Table 6 The factor values for the original descriptors

	Factor 1	Factor 2	Factor 3
p_z	0.141	0.756	-0.613
$(p_x + p_y)/2$	0.981	-0.121	0.133
$1/\Delta E$	0.864		-0.114
NPA	-0.98	-0.179	
σ_I (Taft)		0.943	0.234
r(B-X)	0.665	0.568	-0.101
V_{max}			0.993
Proportion variance	0.448	0.263	0.208
Cumulative variance	0.448	0.711	0.919

■ TOC Graphic

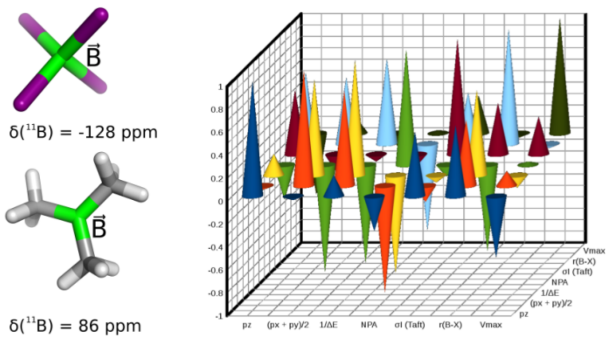

B
δ(11B) = -128 ppm
B
δ(11B) = 86 ppm
1
0.8
0.6
0.4
0.2
0
-0.2
-0.4
-0.6
-0.8
-1
pz
(px + py)/2
1/ΔE
NPA
σI (Taft)
r(B-X)
Vmax